Editors' Suggestion

Rigorous Theory of Coupled Resonators

E. A. Muljarov
School of Physics and Astronomy, Cardiff University, Cardiff CF24 3AA, United Kingdom

(Received 31 May 2025; revised 8 October 2025; accepted 5 December 2025; published 16 January 2026)

We demonstrate the general failure of the famous concept of tight binding and mode hybridization underlying modern theories of coupled open resonators. Despite sophisticated examples in the literature illustrating these theories, they fail to describe planar systems. This includes even the simplest case of two dielectric slabs placed next to each other or separated by a distance, which is straightforward to verify analytically. We present a rigorous theory capable of calculating correctly the eigenmodes of arbitrary three-dimensional dispersive coupled resonators in terms of their individual modes, revealing proper mode hybridization and formation of bonding and antibonding supermodes. Planar optical resonators, such as coupled slabs and Bragg-mirror microcavities, are used for illustration since they allow reliable verification of the theory.

DOI: 10.1103/fqzx-xtl9

Introduction—Any resonator is characterized by its eigenmodes, which can be found by various analytical or numerical methods [1,2]. When two or more open resonators are located next to each other or separated by some distance (top panel in Fig. 1), the modes of each individual resonator are perturbed, and mixing or hybridization of the original eigenstates is expected and in fact observed experimentally, e.g., in photonic molecules [3–11]. It is therefore natural to ask how can these hybrid modes of the coupled resonators be found using the information about the individual resonators, in particular their modes? To address this question, several approaches to finding the modes of coupled optical resonators have been developed [12–16]. However, despite claims that they are rigorous [13] or accurate enough [15], supported by various illustrations [12–16], none of them work even approximately for planar coupled resonators. This is demonstrated in Fig. 1 for the simplest analytically solvable system—a homogeneous dielectric slab made of two identical glass slabs next to each other.

The modes of an electromagnetic system, also known as quasinormal modes or resonant states (RSs), have a simple analytical form in the case of a dielectric slab surrounded by vacuum, with the mode wave numbers

$$k_n = \frac{1}{2a\sqrt{\epsilon}}\left(\pi n - i\ln\frac{\sqrt{\epsilon}+1}{\sqrt{\epsilon}-1}\right), \tag{1}$$

where n is an integer, $2a$ is the slab thickness, and ϵ its permittivity. These wave numbers are the eigenvalues of Maxwell's equations solved with outgoing boundary conditions [17]. They are shown in Fig. 1 for single (black

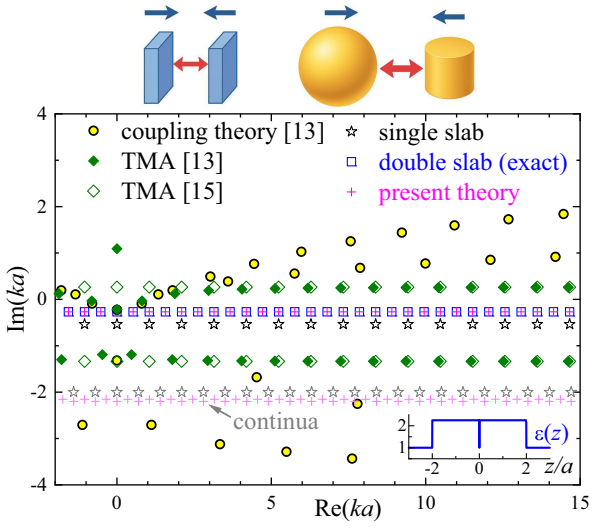

FIG. 1. (Top) Sketches of coupled resonators: Two dielectric slabs (left) and two gold nanoparticles (right), illustrating strong modal interaction (double-sided red arrows) and Casimir forces (blue arrows). (Bottom) RS wave numbers of two identical slabs of width $2a$ and permittivity ϵ next to each other ($d = 0$), calculated exactly (blue open squares), using the coupling theory [13] with a sufficiently number of basis RSs ($N = 3200$) to reach visual convergence (circles), TMAs based on Refs. [13] and [15] (full and open diamonds), and the present theory (magenta crosses) using $N = 100$ basis RSs (black stars) and 150 discretized continuum modes. Gray stars and light-magenta crosses show the continuum modes of the single- and double-slab systems. Inset: permittivity profile of the coupled resonators.

stars) and double slab (blue squares), with the permittivity profile in the inset. Results of the coupling theory [13], using full sets of RSs of each resonator, are also shown (circles), along with a two-mode approximation (TMA) based on [13] and the TMA by Ren *et al.* [15] (open and full diamonds, respectively). Apart from the central ($n = 0$) mode, they are all very different from the exact values Eq. (1), about half having a positive imaginary part, which is unphysical. One could argue that the TMAs fail due to too low quality factor or too short distance between resonators, but this is not the case: these theories also fail for high-quality (high-Q) modes of coupled Bragg-mirror microcavities (MCs). Furthermore, the famous concept of tight binding turns out to be inapplicable to open resonators, as we show in this Letter below.

The fundamental reason why the theories [12–16] fail is that the RSs, though complete within the resonator volume, are *incomplete* outside it, preventing any valid expansion describing the coupling. Recent proposals to fill this gap by RS regularization [18–20] were unsuccessful in developing suitable expansions [21,22], in the best scenario ending in highly nonlinear eigenvalue problems [20] lacking convergence. Completeness outside the resonator has been achieved [23,24] by supplementing physical modes with large sets of unphysical numerical modes from discretization, or with virtual gap modes [25] generated by the resonant-state expansion (RSE) [17]. However, using this completeness for coupled resonators requires an excessively large computational domain [26] and provides no insight into coupling or hybridization.

In this Letter, we develop a rigorous theory of coupled resonators, allowing us to calculate their hybridized modes numerically exactly in terms of the modes of the individual resonators. This is achieved by generalizing the Mittag-Leffler (ML) expansion of the dyadic Green's function (GF) and extending its validity beyond the resonator boundary. The general theory is developed for arbitrary three-dimensional (3D) dispersive resonators, including magnetic or bianisotropic ones. For clarity and verification, illustrations are provided for planar dielectric nondispersive systems, such as two slabs and two MCs separated by a distance. Increasing the distance between resonators, the exponential growth of the RSs imposes serious limitations on the applicability of the theory in a form of poorer or absent convergence. This challenge has been successfully addressed by combining the present theory with the RSE [27] which allows us also to rigorously prove the developed formalism. Moreover, the efficiency of this approach is comparable to that of the RSE, which can be orders of magnitude higher than in existing commercial solvers, as shown in [28].

Two coupled dispersive resonators—Using the notations of Ref. [29], we write Maxwell's equations

$$\nabla \times \mathbf{E} = ik\mathbf{B}, \qquad \nabla \times \mathbf{H} = -ik\mathbf{D} \tag{2}$$

for a monochromatic field with harmonic time dependence $e^{-i\omega t}$ as

$$[k\hat{\mathbb{P}}(\mathbf{r};k) - \hat{\mathbb{D}}(\mathbf{r})]\vec{\mathbb{F}}(\mathbf{r}) = 0, \tag{3}$$

where $k = \omega/c$ is the light wave number,

$$\vec{\mathbb{F}}(\mathbf{r}) = \begin{pmatrix} \mathbf{E}(\mathbf{r}) \\ i\mathbf{H}(\mathbf{r}) \end{pmatrix}$$

is a 6-dimensional vector comprising the electric field $\mathbf{E}$ and magnetic field $\mathbf{H}$, and $\hat{\mathbb{P}}(\mathbf{r};k)$ and $\hat{\mathbb{D}}(\mathbf{r})$ are the generalized dispersive permittivity tensor and curl operator,

$$\hat{\mathbb{P}}(\mathbf{r};k) = \begin{pmatrix} \hat{\boldsymbol{\varepsilon}}(\mathbf{r};k) & \hat{\boldsymbol{\eta}}(\mathbf{r};k) \\ \hat{\boldsymbol{\eta}}^{\mathrm{T}}(\mathbf{r};k) & \hat{\boldsymbol{\mu}}(\mathbf{r};k) \end{pmatrix}, \quad \hat{\mathbb{D}}(\mathbf{r}) = \begin{pmatrix} 0 & \nabla\times \\ \nabla\times & 0 \end{pmatrix}. \tag{4}$$

Here $\hat{\boldsymbol{\varepsilon}}(\mathbf{r};k)$ and $\hat{\boldsymbol{\mu}}(\mathbf{r};k)$ are, respectively, the frequency-dependent 3×3 permittivity and permeability tensors, $\hat{\boldsymbol{\eta}}(\mathbf{r};k)$ is the bianisotropy tensor, and T is transposition. While we assume reciprocity, implying $\hat{\boldsymbol{\varepsilon}}^{\mathrm{T}} = \hat{\boldsymbol{\varepsilon}}$ and $\hat{\boldsymbol{\mu}}^{\mathrm{T}} = \hat{\boldsymbol{\mu}}$, and for illustration use achiral ($\hat{\boldsymbol{\eta}} = 0$) and nonmagnetic systems, generalizations to nonreciprocal systems [24] are straightforward.

Consider two resonators described by $\hat{\mathbb{P}}_1(\mathbf{r};k)$ and $\hat{\mathbb{P}}_2(\mathbf{r};k)$, occupying nonoverlapping volumes V_1 and V_2 [30]. The RSs of the full system, comprising both resonators, are given by Eq. (3) with

$$\hat{\mathbb{P}}(\mathbf{r};k) = \hat{\mathbb{P}}_1(\mathbf{r};k) + \hat{\mathbb{P}}_2(\mathbf{r};k) - \hat{\mathbb{P}}_b, \tag{5}$$

where $\hat{\mathbb{P}}_b$ is the background permittivity (for vacuum, $\hat{\mathbb{P}}_b = \hat{\mathbb{I}}$, where $\hat{\mathbb{I}}$ is the 6×6 identity matrix). The RSs of each resonator satisfy

$$[k_n^{(j)}\hat{\mathbb{P}}_j(\mathbf{r};k_n^{(j)}) - \hat{\mathbb{D}}(\mathbf{r})]\vec{\mathbb{F}}_n^{(j)}(\mathbf{r}) = 0 \tag{6}$$

with outgoing boundary conditions, where n labels the RSs of resonator j. Using the dyadic GF $\hat{\mathbb{G}}_j(\mathbf{r},\mathbf{r}';k)$ of each subsystem, satisfying

$$[k\hat{\mathbb{P}}_j(\mathbf{r};k) - \hat{\mathbb{D}}(\mathbf{r})]\hat{\mathbb{G}}_j(\mathbf{r},\mathbf{r}';k) = \hat{\mathbb{I}}\delta(\mathbf{r}-\mathbf{r}'), \tag{7}$$

the formal solution of Eq. (3) becomes

$$\vec{\mathbb{F}}(\mathbf{r}) = -k\int_{V_2} d\mathbf{r}'\hat{\mathbb{G}}_1(\mathbf{r},\mathbf{r}';k)[\hat{\mathbb{P}}_2(\mathbf{r}';k) - \hat{\mathbb{P}}_b]\vec{\mathbb{F}}(\mathbf{r}') \tag{8}$$

for $\mathbf{r}\in V_1$ and

$$\vec{\mathbb{F}}(\mathbf{r}) = -k\int_{V_1} d\mathbf{r}'\hat{\mathbb{G}}_2(\mathbf{r},\mathbf{r}';k)[\hat{\mathbb{P}}_1(\mathbf{r}';k) - \hat{\mathbb{P}}_b]\vec{\mathbb{F}}(\mathbf{r}') \tag{9}$$

for $\mathbf{r}\in V_2$.

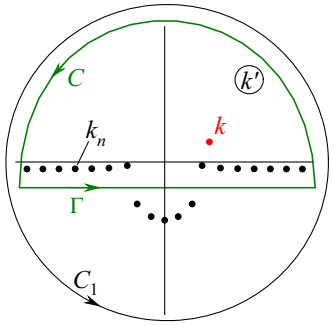

FIG. 2. Full-circle contour C_1, semicircle C, and straight line Γ in the complex k' plane, with the poles $k' = k_n$ of the GF of a resonator and an additional pole at $k' = k$ (red).

To find the wave number k and field $\vec{\mathbb{F}}(\mathbf{r})$ of a RS of the full system, using the RSs of each resonator, one needs to expand the GFs $\hat{\mathbb{G}}_j(\mathbf{r},\mathbf{r}';k)$ in terms of such states. The expansion is the ML series [17,29,31–33]

$$\hat{\mathbb{G}}_j(\mathbf{r},\mathbf{r}';k) = \sum_n \frac{\vec{\mathbb{F}}_n^{(j)}(\mathbf{r}) \otimes \vec{\mathbb{F}}_n^{(j)}(\mathbf{r}')}{k - k_n^{(j)}} \quad \text{for } \mathbf{r},\mathbf{r}' \in V_j, \quad (10)$$

where $\otimes$ denotes the dyadic product. The ML series Eq. (10) converges to the correct GF if both coordinates $\mathbf{r}$ and $\mathbf{r}'$ lie inside V_j. This follows from

$$\lim_{|k|\to\infty} \hat{\mathbb{G}}_j(\mathbf{r},\mathbf{r}';k) = 0 \quad (11)$$

for any complex k and $\mathbf{r},\mathbf{r}' \in V_j$. In fact, the integral of $\hat{\mathbb{G}}_j(\mathbf{r},\mathbf{r}';k')/(k-k')$ over an infinitely large circle in the k' plane (contour C_1 in Fig. 2) is zero, and Cauchy's theorem with Lorentz reciprocity [32] yield Eq. (10), which in turn determines the RS normalization [17,24,28,29,34]. However, Eqs. (8) and (9) require the two GF coordinates to be in different regions, one inside and one outside each resonator. In this case, the ML series Eq. (10) fails, reflecting the incompleteness of RSs outside their resonator. Below we generalize the ML series Eq. (10) beyond the resonator boundary.

Let one of the two coordinates of the GF $\hat{\mathbb{G}}_j$ be outside resonator j, namely, $\mathbf{r}' \notin V_j$ while $\mathbf{r} \in V_j$. Then Eq. (11) holds only in the upper half of the complex k plane, due to outgoing boundary conditions. Integrating $\hat{\mathbb{G}}_j(\mathbf{r},\mathbf{r}';k')/(k-k')$ over the contour in Fig. 2, consisting of an infinite semicircle C [again giving zero due to Eq. (11)] and a straight line Γ [50], we obtain a generalized ML expansion

$$\begin{aligned}\hat{\mathbb{G}}_j(\mathbf{r},\mathbf{r}';k) &= \sum_n \frac{\vec{\mathbb{F}}_n^{(j)}(\mathbf{r}) \otimes \vec{\mathbb{F}}_n^{(j)}(\mathbf{r}')}{k - k_n^{(j)}} - \frac{1}{2\pi i}\int_\Gamma dk' \frac{\hat{\mathbb{G}}_j(\mathbf{r},\mathbf{r}';k')}{k-k'} \\ &= \sum\!\!\!\!\!\!\int_n \frac{\vec{\mathbb{F}}_n^{(j)}(\mathbf{r}) \otimes \vec{\mathbb{F}}_n^{(j)}(\mathbf{r}')}{k - k_n^{(j)}}, \end{aligned} \quad (12)$$

valid for $\mathbf{r} \in V_j$ and $\mathbf{r}' \notin V_j$. Here we use a key property of the GF, proven in [33]: if $\mathbf{r}$ and $\mathbf{r}'$ lie in different regions, then $\hat{\mathbb{G}}_j$ has a factorizable form,

$$\hat{\mathbb{G}}_j(\mathbf{r},\mathbf{r}';k') = -2\pi i \sum_s \vec{\mathbb{A}}_s^{(j)}(\mathbf{r};k') \otimes \vec{\mathbb{B}}_s^{(j)}(\mathbf{r}';k'), \quad (13)$$

where $\vec{\mathbb{A}}_s^{(j)}$ and $\vec{\mathbb{B}}_s^{(j)}$ are vector fields on Γ. These fields complement the RSs $\vec{\mathbb{F}}_n^{(j)}(\mathbf{r})$, with s labeling symmetry channels [52]. Following [32,35], the RSs and continuum modes on Γ are grouped into one set, producing the compact ML form Eq. (12), where the integral accounts for continuum modes and the sum for all the RSs above Γ.

The ML expansion Eq. (12) is exactly what is required to solve Eqs. (8) and (9). However, in dispersive systems, a direct use of Eq. (12) gives a nonlinear eigenvalue problem in k. To linearize it for Drude–Lorentz dispersion [36] of $\hat{\mathbb{P}}_j(\mathbf{r};k)$, we employ alternative GF representations [29,37] alongside Eq. (12), arriving at

$$\vec{\mathbb{F}}(\mathbf{r}) = \begin{cases} \sum\!\!\!\!\!\!\int_n c_n^{(1)} \vec{\mathbb{F}}_n^{(1)}(\mathbf{r}) & \text{for } \mathbf{r} \in V_1, \\ \sum\!\!\!\!\!\!\int_m c_m^{(2)} \vec{\mathbb{F}}_m^{(2)}(\mathbf{r}) & \text{for } \mathbf{r} \in V_2. \end{cases} \quad (14)$$

The coefficients $c_n^{(1)}$, $c_m^{(2)}$ and the RS wave number k satisfy the *linear* eigenvalue problem

$$\begin{aligned}(k - k_n^{(1)})c_n^{(1)} &= -k \sum\!\!\!\!\!\!\int_m U_{nm}^{(2)}(\infty) c_m^{(2)} \\ &\quad + k_n^{(1)} \sum\!\!\!\!\!\!\int_m [U_{nm}^{(2)}(\infty) - U_{nm}^{(2)}(k_n^{(1)})] c_m^{(2)}, \\ (k - k_m^{(2)})c_m^{(2)} &= -k \sum\!\!\!\!\!\!\int_n U_{mn}^{(1)}(\infty) c_n^{(1)} \\ &\quad + k_m^{(2)} \sum\!\!\!\!\!\!\int_n [U_{mn}^{(1)}(\infty) - U_{mn}^{(1)}(k_m^{(2)})] c_n^{(1)}, \end{aligned} \quad (15)$$

with matrix elements

$$\begin{aligned} U_{mn}^{(1)}(q) &= \int_{V_1} d\mathbf{r} \vec{\mathbb{F}}_m^{(2)}(\mathbf{r}) \cdot [\hat{\mathbb{P}}_1(\mathbf{r};q) - \hat{\mathbb{P}}_b] \vec{\mathbb{F}}_n^{(1)}(\mathbf{r}), \\ U_{nm}^{(2)}(q) &= \int_{V_2} d\mathbf{r} \vec{\mathbb{F}}_n^{(1)}(\mathbf{r}) \cdot [\hat{\mathbb{P}}_2(\mathbf{r};q) - \hat{\mathbb{P}}_b] \vec{\mathbb{F}}_m^{(2)}(\mathbf{r}), \end{aligned} \quad (16)$$

see Ref. [33] for details.

Two slabs—We verify the rigorous theory of coupled resonators for two identical dielectric slabs of width $2a$, separated by distance d. For $d = 0$, the eigenvalues k of Eq. (15) (magenta crosses in Fig. 1) agree with the exact solution (blue squares), with the relative error [Fig. 3(a)]

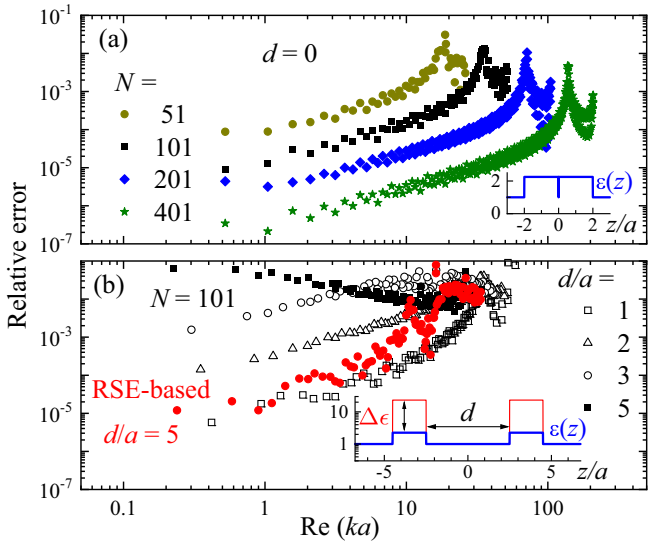

FIG. 3. Relative error for the RS wave numbers of the coupled slab resonators, separated by distance d, calculated by the present theory Eq. (15) with continuum-to-RS ratio $f = 1.5$, (a) for $d = 0$ and the number N of basis RSs as given and (b) for $N = 100$ and d as given, demonstrating the fundamental limitation at large d. The error of the RSE-based approach for $d = 5a$ and $N = 100$ is shown by red circles in (b). Insets: permittivity profiles of the coupled resonators and perturbation $\Delta\epsilon$ used in the RSE-based approach to Eq. (15).

reducing as $1/N^3$, similar to the RSE [17]. Here, N and fN are, respectively, the number of the RSs and discretized continuum modes of an individual resonator, included in Eq. (15) and shown in Fig. 1 by black and gray stars. The discretization affects accuracy similarly to truncation in which only RSs with $|k_n| < k_{\max}(N)$ are kept, so f should ideally grow with N but is fixed here at its optimal value $f = 1.5$.

Increasing the distance d dramatically increases the error [Fig. 3(b)], with large deviations and no convergence already at $d/a = 5$. This originates from the exponential growth of the wave functions outside the resonator [22,38], which fundamentally limits Eq. (15). This limitation is universal, since any resonator has an infinite number of Fabry-Pérot (FP) RSs [39] with large $|\mathrm{Im}\, k_n|$, causing strong exponential increase. We overcome this by combining the above approach with the RSE.

RSE-based approach—The RSE accurately and efficiently finds RSs of a target system using RSs of a basis system [17,28,29,32,38]. Here the target system is a single resonator with average permittivity ϵ, while the basis system has larger permittivity $\epsilon + \Delta\epsilon$, making its FP modes less leaky, $|\mathrm{Im}\, k_n| \sim \gamma_0 \approx (a\Delta\epsilon)^{-1}$, where $2a$ is the shortest size of the basis system. For error reduction the contour Γ (Fig. 2) must lie not far from the real axis and not too close to FP modes. Low-Q modes (e.g., leaky spherical-cavity modes [39]) may remain outside Γ, as illustrated in Fig. 2. Thus the imaginary part of continuum modes on Γ is $\gamma = f_\gamma \gamma_0$, while their exponential growth is limited by $\gamma(d + 2a) = f_d$, giving a distance-dependent perturbation $\Delta\epsilon = (d/a + 2) f_\gamma / f_d$. The constants f_γ and f_d are the two parameters of the theory with optimal values $f_\gamma \approx 12$ and $f_\gamma / f_d \approx 2$, see Ref. [33]. We demonstrate this approach for planar coupled resonators separated by distances up to $d/a = 40$. For two glass slabs in vacuum at $d/a = 5$, the errors [red circles in Fig. 3(b)] for $\Delta\epsilon = 24$ are comparable to the $d = 0$ case without RSE; see Ref. [33] for more results.

The RSE further allows us to rigorously prove the factorizable GF form Eq. (13) and determine the ML expansion Eq. (12) of *any* resonator. Since the GF of a generic resonator is not known analytically, the continua in Eq. (12) would be otherwise inaccessible. However, transforming an analytically solvable resonator into an arbitrary resonator within the RSE preserves Eq. (12) and identifies all contributing modes [33].

Coupled MCs—Applying the RSE-based theory to two $\lambda/2$ MCs, the cavity mode (CM) of a single MC splits by symmetry into three high-Q modes for $d = 0$ [see Fig. 4(a) and right inset], and even more high-Q modes are formed between the MCs for $d = 10.2a$ [Fig. 4(b)]. All the modes of the coupled system are well reproduced by the present theory (magenta crosses) within the shown spectral range, and the error again scales as $1/N^3$ [Fig. 4(c)]; see Ref. [33] for more details and other examples of coupled resonators.

Mapping the expansion Eq. (14) back onto RSs only (no continuum) within each MC where its RSs are complete, $\vec{\mathbb{F}}(\mathbf{r}) = \sum_n b_n^{(j)} \vec{\mathbb{F}}_n^{(j)}(\mathbf{r})$ for $\mathbf{r} \in V_j$, shows mode hybridization and the contribution of all the modes of the singe MC (black crosses x) by red and black circles (with the circle area proportional to $|b_n|^2$), for symmetric (S) and antisymmetric (A) coupled modes [right insets in Figs. 4(a) and 4(b)], for which $b_n = b_n^{(1)} = \pm b_n^{(2)}$ by symmetry. In particular, mode S in Fig. 4(a) and both modes A and S in Fig. 4(b) are dominated by the single CMs, consistent with the field profiles in the left insets, demonstrating mode hybridization. However, using only these dominant contributions, as in tight binding, gives entirely wrong and unphysical splitting as demonstrated by the TMA (green diamonds). Note that the TMA from Eqs. (15) and (16) with one CM per resonator matches the standard tight-binding model.

Figure 4 thus demonstrates that the famous concept of tight binding fails for open coupled resonators, even for high-Q modes [53]. As emphasized in [22], exponential growth causes RSs to increasingly perturb with distance contradicting the intuition that distant objects weakly couple. In the present case of the hybridized bonding and antibonding supermodes, dominated by the CMs, the seemingly small contribution of other RSs (with $|b_n|^2$ below 1% compared to the CMs) cannot be neglected due to their exponential growth and consequently strong coupling between the resonators.

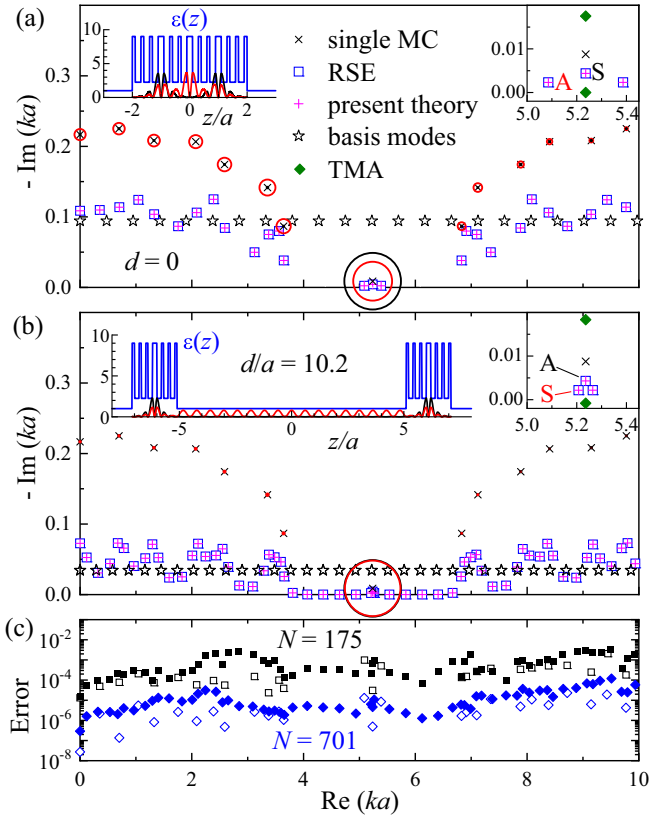

FIG. 4. RS wave numbers of coupled MCs, separated by distance (a) $d = 0$ and (b) $d = 10.2a$, calculated by the RSE [38] (open blue squares) and the present RSE-based theory (magenta crosses +), along with those of a single MC (black crosses) and the basis slab (stars). The expansion coefficients b_n at the single-MC RSs for RSs A and S of the coupled MCs in the right insets are given by the color-coded circles around the single-MC wave numbers, with the circle area $\propto |b_n|^2$. Right insets: zoom around the fundamental CM of the single MC and TMA (green diamonds), demonstrating the failure of tight binding. Left insets: permittivity profiles of coupled MCs (blue) and the electric field $|E|^2$ of the modes S and A (color coded). (c) Relative error for the RSs wave numbers of the coupled MCs in (a) and (b), shown, respectively, by open and full black squares ($N = 175$) and blue diamonds ($N = 701$).

Conclusion—We have developed a rigorous theory of coupled resonators, based on a generalization of the Mittag-Leffler expansion of the dyadic Green's function beyond the resonator boundary, by adding a continuum of modes to the incomplete set of resonant states. To circumvent the fundamental limitation caused by the exponential growth of the resonant states outside a resonator, we have combined this theory with the resonant-state expansion. This provides also a rigorous proof of the formalism and a reliable calculation of the continuum, which are otherwise not possible, since the Green's function of an arbitrary system is not known analytically. We have further shown that the concept of tight binding fails for open resonators, in drastic contrast with recent claims and illustrations [12–16]. The present theory enables calculating, in one run, all eigenmodes within a given spectral range and provides access to important physical applications, such as the Purcell enhancement [34] and Casimir effect [33].

Data availability—The data that support the findings of this article are not publicly available upon publication because it is not technically feasible and/or the cost of preparing, depositing, and hosting the data would be prohibitive within the terms of this research project. The data are available from the authors upon reasonable request.

[1] P. Lalanne, W. Yan, A. Gras, C. Sauvan, J.-P. Hugonin, M. Besbes, G. Demésy, M. D. Truong, B. Gralak, F. Zolla, A. Nicolet, F. Binkowski, L. Zschiedrich, S. Burger, J. Zimmerling, R. Remis, P. Urbach, H. T. Liu, and T. Weiss, Quasinormal mode solvers for resonators with dispersive materials, J. Opt. Soc. Am. A **36**, 686 (2019).
[2] T. Wu and P. Lalanne, Designing electromagnetic resonators with quasinormal modes, Front. Phys. **12**, 1461106 (2024).
[3] M. Bayer, T. Gutbrod, J. P. Reithmaier, A. Forchel, T. L. Reinecke, P. A. Knipp, A. A. Dremin, and V. D. Kulakovskii, Optical modes in photonic molecules, Phys. Rev. Lett. **81**, 2582 (1998).
[4] T. Mukaiyama, K. Takeda, H. Miyazaki, Y. Jimba, and M. Kuwata-Gonokami, Tight-binding photonic molecule modes of resonant bispheres, Phys. Rev. Lett. **82**, 4623 (1999).
[5] S. P. Ashili, V. N. Astratov, and E. C. H. Sykes, The effects of inter-cavity separation on optical coupling in dielectric bispheres, Opt. Express **14**, 9460 (2006).
[6] S. Preu, H. G. L. Schwefel, S. Malzer, G. H. Döhler, L. J. Wang, M. Hanson, J. D. Zimmerman, and A. C. Gossard, Coupled whispering gallery mode resonators in the terahertz frequency range, Opt. Express **16**, 7336 (2008).
[7] Y. Rakovich and J. Donegan, Photonic atoms and molecules, Laser Photonics Rev. **4**, 179 (2010).
[8] M. Benyoucef, J.-B. Shim, J. Wiersig, and O. G. Schmidt, Quality-factor enhancement of supermodes in coupled microdisks, Opt. Lett. **36**, 1317 (2011).
[9] B. Peng, Şahin Kaya Özdemir, J. Zhu, and L. Yang, Photonic molecules formed by coupled hybrid resonators, Opt. Lett. **37**, 3435 (2012).
[10] L. Flatten, A. Trichet, and J. Smith, Spectral engineering of coupled open-access microcavities, Laser Photonics Rev. **10**, 257 (2016).
[11] Y. Li, F. Abolmaali, K. W. Allen, N. I. Limberopoulos, A. Urbas, Y. Rakovich, A. V. Maslov, and V. N. Astratov, Whispering gallery mode hybridization in photonic molecules, Laser Photonics Rev. **11**, 1600278 (2017).
[12] B. Vial and Y. Hao, A coupling model for quasi-normal modes of photonic resonators, J. Opt. **18**, 115004 (2016).
[13] C. Tao, J. Zhu, Y. Zhong, and H. Liu, Coupling theory of quasinormal modes for lossy and dispersive plasmonic nanoresonators, Phys. Rev. B **102**, 045430 (2020).
[14] K. Cognée, in Hybridization of open photonic resonators, Ph.D. dissertation, University of Amsterdam, 2020.

[15] J. Ren, S. Franke, and S. Hughes, Quasinormal modes, local density of states, and classical Purcell factors for coupled loss-gain resonators, Phys. Rev. X **11**, 041020 (2021).
[16] N. Bachelard, A. Schumer, B. Kumar, C. Garay, J. Arlandis, R. Touzani, and P. Sebbah, Coalescence of Anderson-localized modes at an exceptional point in 2D random media, Opt. Express **30**, 18098 (2022).
[17] A. Muljarov, W. Langbein, and R. Zimmermann, Brillouin-Wigner perturbation theory in open electromagnetic systems, Europhys. Lett. **92**, 50010 (2010).
[18] M. I. Abdelrahman and B. Gralak, Completeness and divergence-free behavior of the quasi-normal modes using causality principle, OSA Continuum **1**, 340 (2018).
[19] S. Franke, S. Hughes, M. K. Dezfouli, P. T. Kristensen, K. Busch, A. Knorr, and M. Richter, Quantization of quasinormal modes for open cavities and plasmonic cavity quantum electrodynamics, Phys. Rev. Lett. **122**, 213901 (2019).
[20] P. T. Kristensen, K. Herrmann, F. Intravaia, and K. Busch, Modeling electromagnetic resonators using quasinormal modes, Adv. Opt. Photonics **12**, 612 (2020).
[21] S. Franke, J. Ren, and S. Hughes, Impact of mode regularization for quasinormal-mode perturbation theories, Phys. Rev. A **108**, 043502 (2023).
[22] T. Wu, J. L. Jaramillo, and P. Lalanne, Reflections on the spatial exponential growth of electromagnetic quasinormal modes, Laser Photonics Rev. **19**, 2402133 (2025).
[23] W. Yan, R. Faggiani, and P. Lalanne, Rigorous modal analysis of plasmonic nanoresonators, Phys. Rev. B **97**, 205422 (2018).
[24] C. Sauvan, T. Wu, R. Zarouf, E. A. Muljarov, and P. Lalanne, Normalization, orthogonality, and completeness of quasinormal modes of open systems: The case of electromagnetism, Opt. Express **30**, 6846 (2022).
[25] Z. Sztranyovszky, W. Langbein, and E. A. Muljarov, Extending completeness of the eigenmodes of an open system beyond its boundary, for Green's function and scattering-matrix calculations, Phys. Rev. Res. **7**, L012035 (2025).
[26] In his private communication to the author, Liu confirmed that the coupling theory [13] converges to the exact solution for the example in Fig. 1, if each single-slab problem is treated purely numerically in a domain exceeding the coupled system, and all the numerical modes due to discretization and perfectly matched layers are taken into account.
[27] While the RSE in the presently available literature is not suitable for optical systems on a substrate, there is a prospect that such a geometry can ultimately be treated, for example, by extending the present approach to consider the substrate as a resonator coupled to the optical system.
[28] M. B. Doost, W. Langbein, and E. A. Muljarov, Resonant-state expansion applied to three-dimensional open optical systems, Phys. Rev. A **90**, 013834 (2014).
[29] E. A. Muljarov and T. Weiss, Resonant-state expansion for open optical systems: Generalization to magnetic, chiral, and bi-anisotropic materials, Opt. Lett. **43**, 1978 (2018).
[30] This is a harder case to address from the viewpoint of completeness, since otherwise the RSs of both systems would be complete in the overlap region without adding continua.
[31] J. Bang, F. A. Gareev, M. H. Gizzatkulov, and S. A. Goncharov, Expansion of continuum functions on resonance wave functions and amplitudes, Nucl. Phys. **A309**, 381 (1978).
[32] M. B. Doost, W. Langbein, and E. A. Muljarov, Resonant state expansion applied to two-dimensional open optical systems, Phys. Rev. A **87**, 043827 (2013).
[33] See Supplemental Material at http://link.aps.org/supplemental/10.1103/fqzx-xtl9 for a full derivation of the analytical results of this Letter, optimization of the theory parameters f_γ and f_d, details on numerical calculation, more examples of coupled resonators and comparisons with the TMA, and a general theory of Casimir forces in terms of the RSs; includes Refs. [13,15,17,18,20,25,29,32,34–49].
[34] E. A. Muljarov and W. Langbein, Exact mode volume and Purcell factor of open optical systems, Phys. Rev. B **94**, 235438 (2016).
[35] S. Neale and E. A. Muljarov, Resonant-state expansion for planar photonic crystal structures, Phys. Rev. B **101**, 155128 (2020).
[36] H. S. Sehmi, W. Langbein, and E. A. Muljarov, Optimizing the Drude-Lorentz model for material permittivity: Method, program, and examples for gold, silver, and copper, Phys. Rev. B **95**, 115444 (2017).
[37] E. A. Muljarov and W. Langbein, Resonant-state expansion of dispersive open optical systems: Creating gold from sand, Phys. Rev. B **93**, 075417 (2016).
[38] M. B. Doost, W. Langbein, and E. A. Muljarov, Resonant-state expansion applied to planar open optical systems, Phys. Rev. A **85**, 023835 (2012).
[39] Z. Sztranyovszky, W. Langbein, and E. A. Muljarov, Optical resonances in graded index spheres: A resonant-state-expansion study and analytic approximations, Phys. Rev. A **105**, 033522 (2022).
[40] A. Canós Valero, Z. Sztranyovszky, E. A. Muljarov, A. Bogdanov, and T. Weiss, Exceptional bound states in the continuum, Phys. Rev. Lett. **134**, 103802 (2025).
[41] K. S. Netherwood, H. K. Riley, and E. A. Muljarov, Exceptional points in perturbed dielectric spheres: A resonant-state expansion study, Phys. Rev. A **110**, 033518 (2024).
[42] G. B. Arfken and H. J. Weber, *Mathematical Methods for Physicists, 5th edition* (Academic Press, San Diego, 2001), p. 448.
[43] H. S. Sehmi, W. Langbein, and E. A. Muljarov, Applying the resonant-state expansion to realistic materials with frequency dispersion, Phys. Rev. B **101**, 045304 (2020).
[44] H. Levine and J. Schwinger, On the theory of electromagnetic wave diffraction by an aperture in an infinite plane conducting screen, Commun. Pure Appl. Math. **3**, 355 (1950).
[45] S. V. Lobanov, W. Langbein, and E. A. Muljarov, Resonant-state expansion of three-dimensional open optical systems: Light scattering, Phys. Rev. A **98**, 033820 (2018).
[46] E. A. Muljarov, Full electromagnetic Green's dyadic of spherically symmetric open optical systems and elimination of static modes from the resonant-state expansion, Phys. Rev. A **101**, 053854 (2020).
[47] R. Matloob and H. Falinejad, Casimir force between two dielectric slabs, Phys. Rev. A **64**, 042102 (2001).

[48] M. Levin and S. Rytov, *Theory of Equilibrium Thermal Fluctuations in Electrodynamics* (Science Publishing, Moscow, 1967).
[49] L. D. Landau and E. M. Lifshitz, *Statistical Physics, Part 2*, 4th ed. (Pergamon Press, Oxford, New York, 1980).
[50] A similar integration, though over a finite closed contour is used in the Riesz-projection theory [51].
[51] L. Zschiedrich, F. Binkowski, N. Nikolay, O. Benson, G. Kewes, and S. Burger, Riesz-projection-based theory of light-matter interaction in dispersive nanoresonators, Phys. Rev. A **98**, 043806 (2018).
[52] For example, for a spherically symmetric resonator, s is a combination of the orbital and magnetic quantum numbers (l, m); for a planar system with mirror symmetry, s denotes even- and odd-parity states of the continuum.
[53] This concept may still be working for a subspace of infinite-Q modes, such as bound states in the continuum in coupled photonic-crystal resonators, as recently demonstrated in Ref. [40].